Journal of Molecular Structure (Theochem), 169 (1988) 531-561
Elsevier Science Publishers B.V., Amsterdam — Printed in The Netherlands

STRAIN IN THREE-MEMBERED RINGS CONTAINING SILICON: THE INABILITY OF SILICON TO FORM FLEXIBLE HYBRID ORBITALS*,**

DIETER CREMER*, JÜRGEN GAUSS and ELFI CREMER
Lehrstuhl für Theoretische, Universität Köln, D-5000 Köln 1 (F.R.G.)

(Received 9 December 1987)

ABSTRACT

Energy, geometry, dipole moment, electron density distribution and associated Laplace distribution of trisilacyclopropane (**7**), disilacyclopropane (**8**), disilaaziridine (**9**), disilaoxirane (**10**), disilaphosphirane (**11**), and disilathiirane (**12**) have been calculated at the HF/6-31G(*d*) and MP2/6-31G(*d*) level using HF/6-31G(*d*) geometries. The three-membered ring molecules have been compared with the acyclic reference compounds SiH_3XSiH_3, SiH_3XH and $\overline{Si_2H_5XH}$ ($X=YH_n=SiH_2$, CH_2, NH, O, PH, S) and with the analogous carbon systems $\overline{CH_2XCH_2}$ ($X=CH_2$(**1**), NH(**2**), O(**3**)). The strain energy (SE) of **7** is 11 kcal mol^{-1} larger than that of **1**, which is primarily due to weakening of ring bonds upon bending. Since Si has a lower tendency to hybridize, it does not form sp^n hybrid orbitals with high *p* character needed for optimal bent bonds. The SEs of **7**-**12** increase (decrease) with increasing electronegativity of Y provided Y is a first (second) row atom. These trends are due to changes in bond angle (Baeyer) strain, which in turn depends on the size of Y and the electronegativity difference between Si and Y. For each disila compound investigated, the SE is at least 10 kcal mol^{-1} larger than that of the corresponding C compound. Nevertheless, **7**-**12** should be stable in the absence of electrophilic or nucleophilic agents.

INTRODUCTION

The concept of hybridization introduced by Linus Pauling [1] has proved to be most useful in understanding chemical bonding in highly strained ring compounds. In a small ring with geometrical angles considerably smaller than those of a strain-free acyclic reference compound, hybrid orbitals with high *p* character are formed that allow bond bending and interbond angles larger than the geometrical ones [2,3]. The strength of the bent bonds and, hence, the magnitude of the ring strain depends on the degree of hybridization at the ring

---

* Dedicated to Professor Linus Pauling.

** This work has been presented in part at the Eleventh Austin Symposium on Molecular Structure, Austin TX, March 1986. It is part 21 of the series "Theoretical Determination of Molecular Structure and Conformation".

atoms and the resultant overlap [1]. Estimates on the strain energy (SE) of a ring molecule can be made by establishing a quantitative relationship between the overlap of the hybrid orbitals and the bond energy [1,2].

An alternative approach for determining the SE of a strained ring is based on a dissection of the molecular energy into contributions associated with the various atomic groups of the ring molecule. In this case the SE is equal to the sum of distortion energies which arise when transferring the atomic groups from a strain-free environment into the strained molecule. In this connection one speaks of bond angle strain (Baeyer strain), bond eclipsing strain (Pitzer strain), stretching strain and nonbonded repulsion [2,3].

Although the two descriptions of ring strain are equivalent, it is advisable to utilize both approaches in order to get a detailed insight into the various effects influencing the stability of a strained system. In addition, the second approach can be used to relate strain effects to features of the electron density distribution $\rho(\mathbf{r})$ and to make predictions with regard to their energetic consequences [2]. Such an analysis has been carried out for cyclopropane (**1**) [2]. It revealed that three-membered ring possess peculiar bonding features, which evade classical descriptions and thereby complicate the analysis of ring strain. The peculiarity of **1** had been noted before by Dewar [4]. He pointed out that the chemical and physical properties of **1** were best understood if the six σ-electrons forming the CC bonds are considered to be delocalized in the three-membered ring similar to the six π-electrons in benzene. Hence, he speaks of σ-delocalization and an aromatic stabilization of **1**.

Cremer and Kraka [5,6] added support to the idea of σ-delocalization by analyzing the electron density distribution $\rho(\mathbf{r})$ of **1** and showing that electron density is smeared out over the whole ring surface of the three-membered ring. According to these authors, surface delocalization of σ-electrons increases the stability of **1** by compensating part of its Baeyer and Pitzer strain. Cremer and Gauss [7] showed that σ-electron delocalization in **1** has to do with the existence of a surface orbital. Occupation of this orbital leads to a 2-electron–3-center bond connecting the three C atoms and increasing the electron density in the center of the three-membered ring. The energetic consequences of surface delocalization in **1** were estimated to be stabilizing by 16 kcal mol^{-1} [7].

If one CH_2 group of **1** is replaced by NH or O as in aziridine (**2**) or oxirane (**3**), then the energy of the surface orbital will be lowered and, as a consequence, stabilization of the three-membered ring by surface delocalization should be increased. On the other hand, angle strain increases when going from **1** to **3** due to an increase in the $k(\mathrm{CYC})$ bending constant for $X = YH_n = CH_2$, NH, O. The latter effect can be verified by theoretical calculations or an investigation of the acyclic reference compounds **4**, **5**, and **6** shown in Scheme 1. It seems that the energetic changes in σ-delocalization and Baeyer strain just cancel yielding strain energies for **2** and **3** almost identical with those of **1** [2,5].

Scheme I

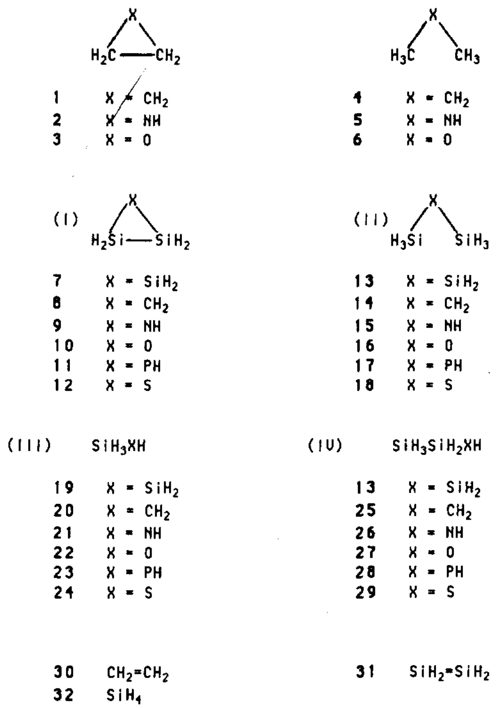

If bonding in a three-membered ring becomes dominated by the surface orbital, the shape of the bent bonds will change. For example, an investigation of the electron density distribution $\rho(\mathbf{r})$ for compounds CH_2XCH_2 ($X=CH_2$(**1**), NH(**2**), O(**3**), OH^+, F^+) revealed that the bending of the CX bonds changes from a convex (outwardly curved) to a concave (inwardly curved) form indicating a continuous transition from a three-membered ring structure to the "T form" of a π-complex for increasing electronegativity of X [5]. Three-membered rings and π-complexes are structurally related [2,5,8]. Systems with concave-shaped bonds are closer to a π-complex than a true ring. A discussion of stability in terms of classical strain theory is no longer valid for these molecules [2]. Nevertheless, it is possible to assess information on bond features, σ-delocalization, and the degree of π-complex character by analyzing $\rho(\mathbf{r})$. An investigation of the electron density in conjunction with a discussion of calculated energies and geometries allows a unified description of structure and stability of three-membered rings and π-complexes [2,5–7].

It is interesting to apply the analysis of $\rho(\mathbf{r})$ to other than carbon rings. Cremer and Gauss [7] have made predictions with regard to the stability of the Si and Ge analogues of **1**. According to these authors, σ-delocalization should be reduced and, hence, the strain energy (SE) of these rings increased. Ab initio calculations on cyclotrisilane (**7**) confirm these predictions [9–12].

Both Sax [9], Schleyer [10], and Nagase and coworkers [12] predict the SE of **7** to be about 10 kcal mol^{-1} larger than that of **1**. Attempts have been made to attribute this increase in SE to a weakening of the SiSi bonds [9] and a concomitant increase in bond angle strain [10]. However, in none of these investigations has a detailed analysis of ring strain considering all possible electronic effects, in particular σ-delocalization, been given. Also, the bent bond character of the SiSi bonds in **7** has not been determined in order to get a detailed account on the structure and stability of **7**.

Another interesting question concerns the degree of π-complex character a three-membered ring containing Si can obtain. How do structure and stability change if one SiH_2 group of **7** is replaced by an atom or group $X=YH_n$ ($n=0$, 1, 2; see Scheme 1, type I compounds **7–12**)? Is there a significant decrease of the bend of the SiY bonds when increasing the electronegativity of Y? An answer to these and related questions is desirable in view of increased efforts to synthesize three-membered rings with two or three Si atoms. So far only highly substituted derivatives of **7** [13–17], disilacyclopropane (**8**) [18–21], disilaoxirane (**10**) [22], and disilathiirane (**12**) [23] are known. However, it is reasonable to also expect stable derivatives of disilaaziridine (**9**) and disilaphosphirane (**11**) [24].

In view of the great interest in three-membered rings containing Si atoms, this work has been carried out to achieve the following goals. First, it is aimed at presenting ab initio energies and geometries of compounds **7–12** (type I, Scheme 1) and to compare these with the acyclic reference compounds SiH_3XSiH_3 (type II), SiH_3XH (type III), and Si_2H_5XH (type IV). For some of these molecules, ab initio investigations have been published [25–30]. But so far no complete set of theoretical data obtained with a basis set of near DZ+P quality has appeared in the literature.

The second aim of this work is to calculate the SEs of **7–12** and to compare them with the SEs of the corresponding C rings, e.g. with those of **1–3**. The comparison is guided by an analysis of the bent bonds, surface delocalization, and the degree of π-complex character of type I compounds. For this purpose the properties of $\rho(\mathbf{r})$ and of its associated Laplace field, $-\nabla^2\rho(\mathbf{r})$ are calculated. On the basis of these calculations predictions with regard to the chemical properties of three-membered rings containing Si are made.

The third and final goal of this work is to trace differences in the stabilities of **7–12** and their C analogues back to the different abilities of Si and C to form flexible hybrid orbitals. We want to test whether the concept of hybridization [1] is sufficient to understand and to predict the thermodynamic and kinetic stabilities of strained ring molecules containing silicon.

METHODS

Calculations have been carried out at the Hartree–Fock (HF) level using the 6-31G(d) basis [31], which contains one set of d-type polarization functions for the heavy atoms. The *d* functions are essential to the description of the bending of the three-membered ring bonds. It is known that HF/6-31G(*d*) leads to reasonable geometries and energies in the case of second row atoms [32]. In order to improve the latter, correlation effects have been considered employing second order Møller-Plesset (MP2) perturbation theory [33]. This level of theory is denoted MP2/6-31G(*d*)//HF/6-31G(*d*), which indicates that MP2 calculations with the 6-31G(*d*) basis have been carried out at HF/6-31G(*d*) geometries.

For type II, III, and IV compounds, the most stable conformation is the one in which adjacent SiH and YH bonds are all staggered (see Fig. 1). In the case of IV with X = NH or PH, it was, a priori, not clear whether the C_s-symmetrical form with XH = YH_cH_t or the C_1-symmetrical form with XH = YH_iH_c is more stable. Therefore, both forms have been optimized and the calculated properties of the more stable one (C_i for X = NH (**26**) and C_s for X = PH (**28**)) have been considered in the discussion.

Ab initio energies have been used to calculate SE for **7–12**. A first estimate

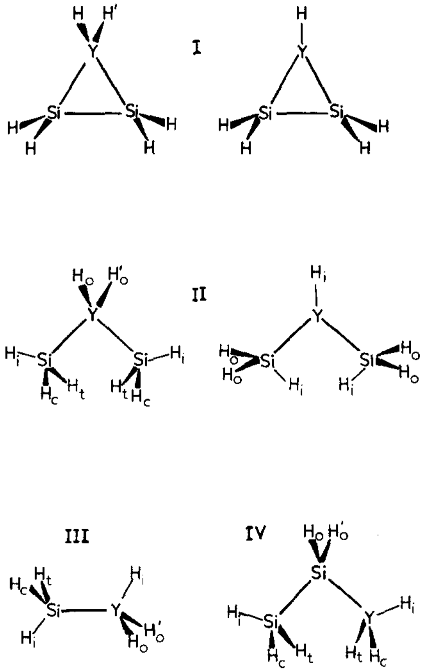

Fig. 1. Conformations of compounds I-IV. H_i and H_o (H_o') denote H atoms in and out of the heavy atom plane. H_c (H_t) is *cis* (*trans*) to H_o. YH_oH_o' = SiH_2 (**7, 13, 19**); CH_2 (**8, 14, 20, 25**); YH_i = NH (**9, 15**); YH_o = NH (**21, 26**); PH (**11, 17, 23, 28**); Y = O (**10, 16, 22, 27**); S (**12, 18, 24, 29**).

of SE has been obtained from the reaction energy $\Delta E(1)$ of the formal reaction (1)

$$+3\ Si_2H_6 \rightarrow H_3SiXSiH_3 + 2\ SiH_3SiH_2SiH_3 \tag{1}$$

The homodesmotic SE [34], which is close to the conventional SE (CSE) defined in thermochemistry, is given by $\Delta E(2)$ of reaction (2)

$$+Si_2H_6 + 2\ SiH_3XH \rightarrow H_3SiXSiH_3 + 2\ SiH_3SiH_2XH \tag{2}$$

By using reaction (1) to get an estimate of SE, energy contributions resulting from bond–bond interactions in $SiH_3SiH_2SiH_3$ (**13**) and SiH_3SiH_2XH are also counted. The latter are measured by the bond separation reactions (3) and (4)

$$SiH_3SiH_2SiH_3 + SiH_4 \rightarrow 2\ SiH_3SiH_3 \tag{3}$$

$$SiH_3SiH_2XH + SiH_4 \rightarrow SiH_3SiH_3 + SiH_3XH \tag{4}$$

If $\Delta E(3)$ and $\Delta E(4)$ are called the bond separation energies (BSE) [35] of **13** and SiH_3SiH_2XH, then the reaction energy of (1) is given by

$$\begin{aligned}\Delta E(1) &= SE(\overline{SiH_2XSiH_2}) + 2\,\{BSE(SiH_3SiH_2XH) - BSE(\mathbf{13})\}\\ &= SE(\overline{SiH_2XSiH_2}) + 2\,\Delta\end{aligned}$$

$\Delta E(1)$ only provides a reasonable estimate for the homodesmotic SE of three-membered rings **7–12** if the BSE of **13** and SiH_3SiH_2XH are similar. In view of the results obtained for the corresponding C compounds [5,35], this should be true for non-polar SiX bonds. In order to test this assumption both sets of reaction energies have been evaluated and compared.

The nature of the ring bonds in **7–12** has been analyzed with the aid of the total electron density distribution $\rho(\mathbf{r})$ and its associated Laplace field $-\nabla^2\rho(\mathbf{r})$. The analysis turned out to be difficult when using the 6-31G(d) or a smaller basis set. It became obvious that one set of d functions is not sufficient to describe the electron density distribution along the bent bonds of three-membered rings containing Si or other second row elements, although computed energies and geometries are reasonable. Therefore, we have used two sets of d functions (6-31G(2d) [36]), one with a larger exponent in order to describe regions closer to the nuclei and one with a smaller exponent (yielding diffuse d functions) in order to describe the region at the center of the bent bonds.

At the HF/6-31G(2d)//HF/6-31G(d) level a reasonable $\rho(\mathbf{r})$ was obtained that could be analyzed along the following lines [5]. First, the paths of maximum electron density (MED paths) between bonded atoms have been determined. Previous investigations have shown that the MED paths are images of the chemical bonds of a molecule and, therefore, can be used to characterize chemical bonds [37]. Each MED path leads through a critical (stationary) point $\mathbf{r}_b$, which is a minimum of $\rho(\mathbf{r})$ along the internuclear connection line and a maximum in all directions perpendicular to this line. Hence, $\rho(\mathbf{r}_b) = \rho_b$ is a saddle point in three dimensions.

A model has been developed to distinguish and characterize covalent, ionic, hydrogen and van der Waals' bonds [38–40]. For this purpose, the energy density $H(\mathbf{r})$ at the saddle point $\mathbf{r}_b$ is analyzed. A value of $H(\mathbf{r}_b) = H_b$ smaller (larger) than zero indicates that electron density at the saddle point $\mathbf{r}_b$ is (de)stabilizing. It has been suggested to consider the existence of a MED path as a necessary and $H_b < 0$ as a sufficient condition for the existence of a covalent bond. If both conditions are fulfilled, we call the MED path "bond path" and the saddle point $\mathbf{r}_b$ "bond critical point" [41].

Bond strength, π-bond character, bond polarity, and bent bond character of covalent bonds can be elucidated from the properties of $\rho(\mathbf{r})$ in the bond, in particular at the bond critical point $\mathbf{r}_b$ [37–40]. The value of ρ_b reflects the strength of the bond. The π-character of a covalent bond can be related to the anisotropy of ρ_b. The latter is measured by the principal curvatures of $\rho(\mathbf{r})$, which in turn are given by the eigenvalues λ_1, λ_2, and λ_3 ($\lambda_1 \leqslant \lambda_2 \leqslant \lambda_3$) of the Hessian matrix of $\rho(\mathbf{r})$. In the case of a bond critical point, λ_1 (strong curvature) and λ_2 (soft curvature) are smaller than 0. The corresponding eigenvectors $\mathbf{v}_i$, which give the direction of the curvature, are perpendicular to the bond path. The curvatures λ_1 and λ_2 are identical for single (σ) bonds with a concentric electron distribution. However, for double bonds the electron distribution is elliptic as reflected by the bond ellipticity $\epsilon_b = \lambda_1/\lambda_2 - 1$. The value of ϵ describes the π-bond character of the bond, the direction of the soft curvature $\mathbf{v}_2$ defines the π direction [37].

The bond path does not necessarily coincide with the internuclear axis. Hence, the bond path length R_b can be larger or equal to the calculated internuclear distance R_e. If one considers the bond paths as a result of atom–atom interactions and their geometrical location as the best energetic compromise between stabilizing and destabilizing forces exerted on the electrons, then it seems reasonable to discuss bond lengths in terms of R_b rather than in terms of R_e. The same holds for the bond angles. The geometrical angle α is in a chemical sense less meaningful than the interpath angle β. In the case of strained molecules β can differ considerably from α. This is important when estimating Baeyer strain by Hooke's law [2,5–7]. The bent bond character is quantitatively assessed by the ratio $Q = (R_b/R_e - 1)1000$, by the perpendicular distance d between $\mathbf{r}_b$ and the internuclear connection line, and by the interpath angle β.

Surface delocalization of electrons in three-membered rings is reflected by the properties of $\rho(\mathbf{r})$ at the ring critical point $\mathbf{r}_r$. There, $\rho(\mathbf{r})$ is a minimum in the ring plane, but a maximum in the direction perpendicular to the ring plane [37]. The ratio $\eta = (\rho_r/\rho_b)100$, where $\rho_r = \rho(\mathbf{r}_r)$ and ρ_b is the average of the three ρ_b values, gives the extent of electron density in the ring plane [5]. Useful insights into the distribution of electrons in the ring plane are also given by the ellipticity $\epsilon(\mathbf{r}_b) = \epsilon_r$ and the Laplace distribution $\nabla^2\rho(\mathbf{r})$. The latter is given by the sum of the eigenvalues λ_i of the Hessian matrix at a point $\mathbf{r}$. A negative (positive) value of $\nabla^2\rho(\mathbf{r})$ is indicative of local charge concentration (depletion) [42,43]. Contour line diagrams of the Laplace concentration $-\nabla^2\rho(\mathbf{r})$ reveal where electrons concentrate in the internuclear regions. Regions of concentration of $\rho(\mathbf{r})$ can be assigned to electron bonding and electron lone pairs. They can also be related to the shape of the frontier orbitals [44].

RESULTS

Since energies and geometries for **1–6** have been published recently [5], only results for Si-containing molecules are tabulated in this work. In Table 1 calculated HF/6-31G(*d*) and MP2/6-31G(*d*) energies for compounds **7–32** are listed. The corresponding HF/6-31G(*d*) geometries are given in Tables 2 (type I compounds), 3 (II), 4 (III), and 5 (IV). Figure 1 explains the notation used for the geometrical parameters. It also displays the most stable conformations of II, III, and IV. In Table 6, computed geometries of I–IV are compared. Experimental geometries of compounds related to **7–12** are shown in Table 7. Features of the computed electron density distribution in **7–12** are summarized in Tables 8 and 9. Finally, in Table 10 computed SEs are listed and analyzed.

Geometries

A comparison of computed geometries for **7–12** with experimental data is difficult since only the geometries of some highly substituted derivatives of **7**, **8**, and **12** are known (see Table 7). SiSi bond distances in alkyl substituted cyclotrisilanes vary from 2.38 to 2.51 Å where a distinct dependence on the bulk of the substituents and, hence, on the degree of steric repulsion can be observed [45]. Extrapolating the data summarized in Table 7, an experimental *R*(SiSi) of 2.34 Å for **7** (Table 2) seems to be reasonable. The same holds for the experimental and computed *R*(SiSi) values of **8**, **12** and their derivatives (Table 2 and 7). The corresponding *R*(SiX) values, which should only indirectly depend on steric interactions between the substituents at the Si atoms, agree within 0.004 Å. We conclude that the ab initio geometries presented in Table 2 are reasonable. In the following we concentrate on a comparison of geometries obtained for I and reference compounds II–IV (Scheme 1).

Calculated SiSi distances in three-membered rings **7–12** are smaller than those of their acyclic counterparts III while the SiY (Si≠Y) distances are similar or slightly longer than that of either II, III or IV. The SiSi distance

TABLE 1

Calculated energies for three-membered rings **7**–**12**, bissilyl compounds **13**–**18**, silyl compounds **19**–**24**, and disylyl compounds **25**–**29**, silene (**31**), and silane (**32**)[a]

Molecule	HF/6-31G(*d*)//HF/6-31G(*d*)	MP2/6-31G(*d*)//HF/6-31G(*d*)
 (I)		
7 X=SiH_2	−870.18218	−870.45481
8 X=CH_2	−619.13561	−619.45458
9 X=NH	−635.16696	−635.51686
10 X=O	−655.02245	−655.38732
11 X=PH	−921.42986	−921.72599
12 X=S	−977.68446	−977.99458
 (II)		
13 X=SiH_2	−871.38646	−871.65628
14 X=CH_2	−620.35166	−620.66825
15 X=NH	−636.38767	−636.73334
16 X=O	−656.25902	−656.61531
17 X=PH	−922.62373	−922.91633
18 X=S	−978.87537	−979.18194
SiH_3XH (III)		
19 X=SiH_2	−581.30509	−681.48489
20 X=CH_2	−330.27241	−330.50022
21 X=NH	−346.28394	−346.54213
22 X=O	−366.13040	−366.40286
23 X=PH	−632.53497	−632.73731
24 X=S	−688.77072	−688.98857
SiH_3SiH_2XH (IV)		
25 X=CH_2	−620.35098	−620.66806
26 X=NH, C_s	−636.36042	−636.70777
C_1	−636.36175	−636.70905
27 X=O	−656.20828	−656.56933
28 X=PH, C_s	−922.61550	−922.90806
C_1	−922.61514	−922.90754
29 X=S	−978.85018	−979.15758
31 Si_2H_4	−580.07664	−580.25863
32 SiH_4	−291.22513	−291.30703

[a] Absolute energies in hartree.

TABLE 2

HF/6-31G(*d*) geometries of three-membered rings **7**-**12** and silene (**31**)[a]

	Symm.	*R*(SiSi)	*R*(SiY)	*R*(SiH)	*R*(YH)	HSiH	(SiSi)YH	(HH)SiSi
7 X=SiH_2	D_{3h}	2.341		1.474		112.8	123.6	150.0
8 X=CH_2	C_{2v}	2.255	1.910	1.471	1.082	112.4	124.5	162.7
9 X=NH	C_{2v}	2.233	1.731	1.475	0.996	108.6	180.0	167.1
10 X=O	C_{2v}	2.196	1.687	1.470		110.0		173.1
11 X=PH[b]	C_s	2.277	2.285	1.470	1.406	113.1	97.1	154.6
				1.469				160.6
12 X=S	C_{2v}	2.254	2.157	1.469		111.8		161.5
31 Si_2H_4	D_{2d}	2.126		1.467		115.4		180.0

[a] Bond lengths are given in Å, angles in degree. (AA) defines the midpoint of the line AA. For C_s symmetry (AA) is given by the projection of A into the SiYSi plane. [b] For **11** the first entry corresponds to the H atom *cis* to PH, the second to the H atom *trans* to PH. Calculated angles are: SiSiH(*cis*) 119.8; SiSiH(*trans*) 121.4; PSiH(*cis*) 116.9; PSiH(*trans*) 114.7; HPSiH(*cis*) 17.0; HPSiH(*trans*) 153.1°.

TABLE 3

HF/6-31G(*d*) geometries of $X(SiH_3)_2$ compounds **13**-**18**[a]

$H_3SiXSiH_3$ X=YH_n	Symm.	*R*(SiY)	*R*(SiH_i)	*R*(SiH_0)	*R*(YH)	SiYSi	(SiSi)YH	H_iSiY	(H_0H_0)SiY	H_0SiH_0
13 X=SiH_2	C_{2v}	2.357	1.478	1.478	1.481	112.8	126.2	110.7	126.2	108.3
14 X=CH_2	C_{2v}	1.888	1.478	1.478	1.089	116.4	126.9	110.7	126.7	108.4
15 X=NH[b]	C_{2v}	1.733	1.473	1.478	1.003	130.9	180.0	108.1	128.4	106.9
16 X=O	C_{3v}	1.626	1.473	1.474		169.9		109.6	126.2	108.9
17 X=PH[c]	C_s	2.263	1.474	1.476	1.404	101.8	103.1	108.6	125.4	108.9
				1.475					129.7	
18 X=S	C_{2v}	2.149	1.469	1.473		104.1		106.2	127.2	108.5

[a] Bond lengths are given in Å, angles in degree. (AA) defines the midpoint of the line AA. For C_s symmetry point (AA) is given by the projection of A into the SiYSi plane. [b] The SiH bonds are staggered with regard to the NH bond (see Fig. 1). [c] For **17** the first entry corresponds to the H atom *cis* to PH, the second to the H atom *trans* to PH. H_i is not exactly in the SiPSi plane, but *cis* with regard to the PH bond. Calculated angles are: PSiH(*cis*) 113.3; PSiH(*trans*) 107.5; H_iSiPSi 173.9; HPSiH(*cis*) 52.7; HPSiH(*trans*) 62.7°.

decreases in the series **7**, **11**, **12**, **8**, **9**, **10** (Table 6), which suggests that the SiSi distance depends on the electronegativity of Y (see below). For the most electronegative Y, namely O, the SiSi distance in I is 0.148 Å shorter than that in III and just 0.078 Å longer than that of disilene (Table 2).

A short SiSi bond distance may also be caused by geometrical constraints resulting from the size of the atom Y at the apex of the ring. For example, in the acyclic reference compounds II, III, and IV the SiY bond distance is always smaller than the SiSi bond distance (Tables 3–5). In a three-membered ring

TABLE 4

HF/6-31G(d) geometries of SiH_3XH compounds **19–24**[a]

Parameter	**19**	**20**	**21**	**22**	**23**	**24**
	X=SiH_2	X=CH_2	X=NH[b]	X=O	X=PH[b]	X=S
Symmetry	D_{3d}	C_3	C_s	C_s	C_s	C_s
R(SiY)	2.352	1.888	1.724	1.648	2.266	2.151
$R(SiH_i)$	1.478	1.478	1.482	1.469	1.476	1.470
$R(SiH_o)$			1.475	1.477	1.475	1.472
$R(YH_i)$		1.086		0.946		1.329
$R(YH_o)$			0.998		1.404	
$YSiH_i$	110.4	110.6	115.5	106.8	113.4	105.0
$YSiH_o$			108.2	111.5	108.0	111.2
H_oSiH_o		108.3	110.4	107.6	109.3	108.8
$SiYH_i$		111.1		118.9		98.1
$SiYH_o$			120.6		97.4	
H_iSiYH_i	180	180		180		180
H_iSiYH_o	60	60	73.2		48.3	

[a] Bond lengths are given in Å, angles in degree. [b] Calculated angles HYH and (HH)YSi are: 111.0; 154.0 (N); 95.6; 101.0° (P).

this implies (geometrical) angles α(SiSiY) smaller and angles α(SiYSi) larger than 60° (see Table 8). In order to avoid a strong increase in Baeyer strain for small α, the SiY (SiSi) distances are elongated (reduced): the larger this effect, the smaller the covalent radius of Y and, hence, α(SiSiY). In line with this interpretation, the smallest α(SiSiY) and the largest increase of the SiY distance (Table 6) is found for O while deviations Δ are relatively small for Y=P or S (Table 6 and Fig. 2(a)).

The only exception is found for X=NH. There, the SiN distance is shorter and $\Delta\alpha$ larger than expected in view of the Δ-values observed for **8** and **10**. It seems that this is a consequence of the geometry at the N atom of **9**. Contrary to aziridine (**2**), which has the NH bond bent by 65° out of the ring plane [5], the NH bond of **9** lies in the plane thus leading to a C_{2v} symmetrical molecule. Since planarity at the N atom implies sp^2 hybridization and, accordingly, an increase of α(SiYSi) (see Tables 6 and 8), the Baeyer strain of the ring should be considerably increased. Of course, the geometrical effect caused by the size of N (vide infra) facilitates a widening of α(SiYSi). In addition, there seem to be electronic effects, which enforce the planar geometry. For example, similar geometrical arrangements at the N atom have been found for the acyclic silylamins **15** (planarity at N, see Fig. 1), **21** (angles SiN(HH)=154.0°; SiNH=120.6°), and **26** (SiN(HH)=153.8°; SiNH=120.6°, see Tables 3–5 and refs. 26, 28 and 29). They are related to the SiOSi and SiOH angle widening found for disiloxane **16** (angle SiOSi=143° [46]), silanol **22**

TABLE 5

HF/6-31G(d) geometries of SiH_3SiH_2XH compounds **25–29**[a,b]

Parameter	**25**	**26**		**27**	**28**		**29**
	X=CH_2	X=NH[c]		X=O	X=PH[c]		X=S
Symmetry	C_s	C_s	C_1^d	C_s	C_s	C_1^d	C_s
R(SiSi)	2.355	2.359	2.350	2.344	2.354	2.355	2.352
R(SiY)	1.895	1.732	1.733	1.656	2.276	2.274	2.161
R(SiH$_i$)	1.479	1.481	1.480	1.480	1.478	1.478	1.478
R(SiH$_c$)	1.480	1.482	1.481	1.478	1.478	1.478	1.476
R(SiH$_t$)			1.478			1.477	
R(SiH$_o$)	1.481	1.478	1.486	1.481	1.478	1.479	1.476
R(SiH$_o'$)			1.478			1.478	
R(YH$_i$)	1.086		0.999	0.947		1.404	1.329
R(YH$_c$)	1.086	0.998	0.998		1.404	1.404	
SiSiY	112.1	115.5	109.4	107.8	114.8	110.5	108.0
SiSiH$_i$	110.8	111.1	110.3	109.1	110.8	110.0	108.6
SiSiH$_c$	110.8	111.0	110.6	111.0	110.0	110.2	110.4
SiSiH$_t$			111.3			110.4	
H$_c$SiH$_t$	108.0	107.6	108.1	108.9	108.5	108.6	109.3
SiSiH$_o$	108.8	108.3	108.2	110.5	110.1	109.8	110.7
SiSiH$_o'$			110.7			109.7	
YSiH$_o$	109.8	107.7	114.9	110.8	106.8	112.1	109.9
YSiH$_o'$			107.3			106.7	
H$_o$SiH$_o'$	107.3	109.1	106.4	108.4	108.1	107.4	107.6
SiYH$_i$	110.9		119.6	118.7		97.3	98.2
SiYH$_c$	111.2	120.6	120.3		97.6	97.5	
H$_c$SiSiY	59.9	59.8	57.7	60.6	59.8	60.2	60.5
H$_t$SiSiY			−62.5			−59.9	
SiSiYH$_i$	180		167.0	180		−168.0	180
SiSiYH$_c$	−60.1	−73.1	−50.2		−48.3	−71.2	

[a]Bond lengths are given in Å, angles in degrees. [b]The following conformations have been calculated (see IV in Fig. 1): **25**: YH$_c$H$_t$H$_i$; **26** (C_s), **28** (C_s): YH$_c$H$_t$; **26** (C_1), **28** (C_1): YH$_c$H$_i$; **27**, **29**: YH$_i$. [c]Calculated angles HYH and (HH)YSi are: 111.0; 153.8 (**26**, C_s); 110.4; 151.0 (**26**, C_1); 95.5; 101.4 (**28**, C_s); 95.6; 101.1° (**28**, C_1). [d]H$_i$ at Si and H$_i$ at Y are both not exactly in the heavy atom plane: YSiSiH$_i$: 177.1 (N); 179.9 (P); H$_o$SiSiH$_i$: 51.4 (N); 55.8 (P); H$_o'$SiSiH$_i$: −64.8 (N); −62.7 (P); H$_o$SiYH$_i$: −71.2 (N); −45.1 (P); H$_o'$SiYH$_i$: 46.8 (N); 72.8° (P).

(SiOH=118.9°), and disilanol **27** (SiOH=118.7°, see Tables 3–5 and ref. 30). These geometrical features have been interpreted in terms of d_π–p_π conjugation and ionic character of the SiY bond (see, e.g. the discussion in ref. 26). Therefore, it will be interesting to investigate angle widening at N and O in the light of the electron density distribution calculated for molecules **9**, **15**, **16**, **21**, **22**, **26**, and **27**.

External ring bonds of **7–12** are slightly shorter than those of the reference

TABLE 6

Comparison of bond lengths and bond angles of compounds I-IV[a]

Molecule	$\Delta(\text{Si-Si})_{IV}$	$\Delta(\text{Si-Y})_{IV}$	$\Delta(\text{Si-Y})_{III}$	$\Delta(\text{Si-Y})_{II}$	Δ(SiYSi)	Δ(SiSiY)	$\Delta(\text{Si-H})_{IV}$	$\Delta(\text{Y-H})_{II}$
7 $X=SiH_2$	−16	−16	−11	−16	0	0	−7	−7
8 $X=CH_2$	−100	15	22	22	12.4	−6.2	−10	−7
9 X=NH	−117	−2	7	0	20.3	−10.2	−11, −3	−7
10 X=O	−148	31	39	61	21.2	−10.6	−11	
11 X=PH	−77	9	6	22	−0.2	0.1	−8	2
12 X=S	−98	−4	6	8	13.0	−1.5	−7	

[a] Compare with Scheme 1. Δ gives the deviation of the bond lengths of type I compounds from those of type II-IV compounds in $\text{Å}\cdot10^3$. In the case of IV, the most stable conformation is compared. For bond angles, Δ measures the deviation from $\alpha=60°$.

TABLE 7

Experimentally determined geometries of three-membered ring compounds containing silicon[a]

Molecule	Substituents	Si-Si	Si-Y	SiYSi	SiSiY	Reference
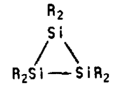	R: t-Butyl	2.511		60		16
	R′: t-Butyl R″: Mesityl	2.428* 2.416*	(*cis-cis*) (*cis-trans*)	60* 60*		17
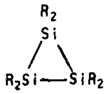	R: 2,6-Dimethylphenyl	2.407*		60*		13
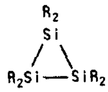	R: CH_2-t-butyl	2.376*		60*		15
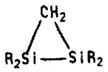	R: 2,6 Dimethylphenyl	2.272	1.887	74.1	53.0	20
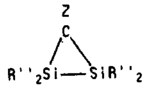	Z: =C (Phenyl) SiH_3 R′: Phenyl R″: Mesityl	2.327	1.907*	75.2	52.4*	19
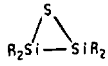	R: Mesityl	2.289	2.161	64.0	58.0	22

[a]Bond lengths in Å, angles in degree. Asterisks indicate averaged values.

compounds III. This has also been found for the analogue C rings and is of relevance when assessing the stability of the ring (see discussion in refs. 2 and 7).

Energies

HF/6-31G(d) values of the homodesmotic SEs calculated with the aid of reaction (2) differ by 1–2 kcal mol^{-1} from the corresponding MP2 values (Table 10). This difference is acceptable considering the fact that for both sets of calculations HF/6-31G(d) geometries have been used. Reaction energies $\Delta E(1)$ are, apart from $X = PH$, 2–6 kcal mol^{-1} larger than energies $\Delta E(2) = SE$. Since $\Delta E(1)$ comprises SE and BSEs (vide infra), this is indicative of a difference in interaction energies between two SiSi bonds on the one side and a SiY and a SiSi bond on the other side.

TABLE 8

Properties of energy and electron density of compounds **1–3**, **7–12** and compound **31**[a]

Molecule	Pauling $\chi(Y)$[b]	ρ_b	$\nabla^2\rho_b$	H_b	R_b	Q	d	α	β
C-C bond								*CCY*	
1 $X=CH_2$	2.55	1.642	−10.199	−1.277	1.507	6.7	0.058	60	78.7
2 $X=NH$	3.04	1.720	−11.873	−1.404	1.487	10.9	0.079	59.5	77.3
3 $X=O$	3.44	1.779	−13.320	−1.510	1.475	15.1	0.093	58.8	73.0
C-Y bond								*CYC*	
2 $X=NH$		1.803	−15.098	−1.969	1.454	3.5	0.008	61.0	75.3
3 $X=O$		1.789	−10.436	−2.793	1.404	2.1	0.039	62.4	75.6
Si-Si bond								*SiSiY*	
7 $X=SiH_2$	1.90	0.598	−3.098	−0.279	2.368	11.5	0.150	60.0	81.7
8 $X=CH_2$	2.55	0.604	−3.143	−0.296	2.332	34.1	0.243	53.8	77.1
9 $X=NH$	3.04	0.601	−3.146	−0.296	2.349	51.9	0.299	49.8	76.2
10 $X=O$	3.44	0.611	−3.194	−0.312	2.330	61.0	0.316	49.4	73.7
11 $X=PH$	2.19	0.630	−3.436	−0.311	2.317	17.6	0.176	60.1	78.3
12 $X=S$	2.58	0.643	−3.603	−0.324	2.308	23.9	0.203	58.5	76.3
$SiH_2=SiH_2$	1.90	0.734	−4.398	−0.434	2.126				
Si-Y bond								*SiYSi*	
8 $X=CH_2$		0.750	4.571	−0.470	1.915	2.6	0.059	72.4	83.9
9 $X=NH$		0.818	14.541	−0.342	1.735	2.3	0.043	80.3	96.8
10 $X=O$		0.829	19.339	−0.240	1.687	0	0.003	81.2	79.2
11 $X=PH$		0.605	−1.171	−0.408	2.297	5.3	0.069	59.8	78.2
12 $X=S$		0.613	2.547	−0.373	2.163	6.5	0.032	63.0	77.3

[a] ρ_b in e Å^{-3}, $\nabla^2\rho_b$ in e Å^{-5}, H_b in hartree Å^{-3}, R_b and d in Å, α and β in deg, and Q in 1/1000.
[b] Pauling scale of electronegativity χ; values from A.E. Allred, J. Inorg. Nucl. Chem., 17 (1961) 215.

The HF/6-31G(d) BSE of **13** is 0.9 kcal mol^{-1} (Table 10) indicative of small stabilizing bond–bond interactions. The experimental BSE is 1.1 kcal mol^{-1} using the experimental ΔH_f^0 values for **13** (28.9), **19** (19.1), and **32** (8.2 kcal mol^{-1} [47]). BSE values for type IV compounds are negative for $X=CH_2$, NH, O, but positive or close to zero for PH and S. The same trends have been found for the BSEs of SiH_3CH_2XH [32]. It is probably due to a destabilization of the SiSi bond by first row substituents, which is not compensated by anomeric interactions typical for the corresponding C compounds [32]. The BSEs of type II compounds also shown in Table 10 are positive

TABLE 9

π-character of bonds and degree of surface delocalization for compounds **1**–**3**, and **7**–**12**

Molecule	$\epsilon(SiSi)_b$	$\epsilon(SiY)_b$	ϵ_r	Direction of $v_{2,r}$	ρ_b	η	$\nabla^2\rho_b$
1 $X=CH_2$	0.455	0.455	0		1.331	81.1	3.843
2 $X=NH$	0.345	0.411	0.357	II	1.425	80.3	6.253
3 $X=O$	0.265	0.705	0.891	II	1.468	82.2	9.056
7 $X=SiH_2$	0.328	0.328	0		0.427	71.4	0.669
8 $X=CH_2$	0.359	0.358	2.664	II	0.540	77.0	0.311
9 $X=NH$	0.185	0.037	8.062	II	0.539	72.3	1.314
10 $X=O$	0.312	0.089	44.403	II	0.567	75.0	0.532
11 $C=PH$	0.379	0.557	0.700	II	0.483	78.7	0.529
12 $X=S$	0.275	0.384	2.502	II	0.509	81.7	0.877

[a] ρ_b in $e\cdot Å^{-3}$, $\nabla^2\rho_b$ in $e\cdot Å^{-5}$. [b] Direction v of major axis of ϵ_r is either parallel (II) or perpendicular (I) to the basal CC or SiSi axis.

TABLE 10

Isodesmic and homodesmotic reaction energies. Analysis of ring strain in terms of angle compression[a]

Parameter	**7** $X=SiH_2$	**8** $X=CH_2$	**9** $X=NH$	**10** $X=O$	**11** $X=PH$	**12** $X=S$
$-\Delta E(1)$						
HF/6-31G(*d*)	38.9	46.3	49.2	59.2	32.3	30.5
MP2/6-31G(*d*)	37.3	45.0	46.7	53.9	30.2	28.5
BSE(IV)						
HF/6-31G(*d*)	0.9	−0.9	−2.2; −1.4	−1.3	0.4; 0.6	−0.3
MP2/6-31G(*d*)	−4.1	−6.3	−7.7; −6.9	−7.2	−4.5; −4.2	−5.6
BSE(II)						
HF/6-31G(*d*)	0.9	1.3	2.6	5.6	1.1	0.8
$SE=-\Delta E(2)$						
HF/6-31G(*d*)	38.9	42.7	43.0; 41.3	54.7	31.3; 30.7	28.1
MP2/6-31G(*d*)	37.3	40.5	39.5; 37.9	47.7	29.5; 30.2	25.4
Δ(SiYSi)	31.1	32.5	34.1	62.9[b]	23.6	26.8
2Δ(SiSiY)	62.2	70.0	78.6; 66.4	68.2	73.0; 64.4	63.4
ΣΔ	93.3	102.5	112.7; 100.5 106.6[c]	131.1	96.6; 88.0 92.3[c]	90.2

[a] Energies of reaction (1) bond separation energies for type IV and II compounds (reaction (3)) and homodesmotic strain energies (reaction (2)) in kcal mol^{-1}. Δ(SiYSi) = β(II) − β(I) and Δ(SiSiY) = β(IV) − β(I) in degree. ΣΔ = Δ(SiYSi) + 2Δ(SiSiY). In case of two entries, the first corresponds to the C_s, the second to the C_1 conformation of type IV compounds (see text). [b] For disiloxane, the experimental SiOSi angle has been used. See ref. 46. [c] Averaged ΣΔ values.

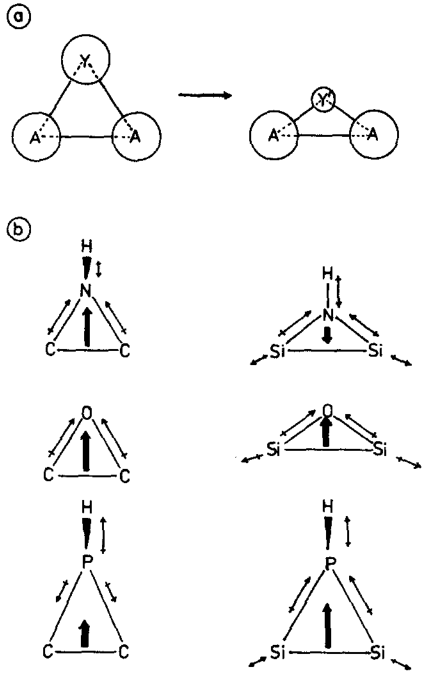

Fig. 2. (a) Geometrical distortions of a three-membered ring containing the second row atoms A and Y upon incorporation of a first row atom Y' ($A=Si$; $Y=Si, P, S$; $Y'=C, N, O$). The geometrical angle $\alpha(AYA)$ increases, angles $\alpha(AAY)$ decrease. (b) Analysis of dipole moments μ (heavy arrows) in terms of bond dipoles (light arrows). The arrow head indicates the negative end of μ. For $\mu > 0$ ($\mu < 0$), it points toward Y (the Si,Si midpoint).

indicating that SiY, SiY interactions are stabilizing despite unfavorable electrostatic interactions between the silyl groups.

The SE values of **7**, **8**, **9**, and **10** are 11, 15, 11 and 23 kcal mol^{-1} larger than the calculated SE of **1**, **2**, and **3**, respectively [5]. Obviously, a replacement of C by Si leads to a significant destabilization of the three-membered ring. While the SEs of **1**, **2**, and **3** are all close to 27 kcal mol^{-1}, that of **7** increases considerably when going from **7** to **10** (CH_2, 3.8; NH, 4.1; O, 15.8 kcal mol^{-1}, see Table 10). This may have to do with the geometrical distortions of the three-membered ring upon incorporating a much smaller first row atom. For example, when replacing one SiH_2 group by a group with another second row atom, the SE decreases ($X=PH$: -7.6; $X=S$: -10.8 kcal mol^{-1}, Table 10). The dependence of SE on the nature of X has to be investigated in more detail in the next chapters.

Dipole moments

HF/6-31G(d) dipole moments μ are normally 10–20% too large due to a tendency of the 6-31G (d) basis to overestimate charge separation in polar bonds

[32]. This has to be borne in mind when analyzing the calculated μ values listed in Table 11. They increase in magnitude from **7** to **12** (Table 11). The same holds for type II compounds. The direction of μ is parallel to the C_2 or C_s symmetry element in I and II, pointing with its negative end either toward X ($\mu > 0$) or toward (SiSi), the midpoint of the Si, Si connection line ($\mu < 0$; X$=$CH$_2$, NH). Magnitude and direction of μ can be rationalized by summing over bond dipole moments as shown schematically in Fig. 2(b). For example, contributions of bond dipoles $Si^{\delta+}H^{\delta-}$ and $N^{\delta-}H^{\delta+}$ are larger than those of $Si^{\delta+}N^{\delta-}$ bond dipoles thus yielding a small negative μ (Table 11). Since the

TABLE 11

HF/6-31G(*d*) dipole moments and ionization potentials[a]

Molecule	μ	μ(C)[b]	Nature of HOMO	*I*
7 X$=$SiH$_2$	0	0	σ(SiSi)	9.03
8 X$=$CH$_2$	−0.26		σ(SiSi)	8.92
9 X$=$NH	−0.56	1.90	σ(SiSi)	9.45
10 X$=$O	1.82	1.89	σ(SiSi)	9.38
11 X$=$PH	1.72	1.12	σ(SiSi)	8.62
12 X$=$S	2.53	1.85	σ(SiSi)	9.52
13 X$=$SiH$_2$	−0.04	0.08	σ(SiSi)	10.45
14 X$=$CH$_2$	−0.79		σ(SiSi)	11.75
15 X$=$NH	−0.90	1.03	*n*(N)	10.62
16 X$=$O	0.14[c]	1.30	*n*(O)	12.11
17 X$=$PH	1.12	1.23	*n*(P), σ(SiP)	9.51
18 X$=$S	1.70	1.50	*n*(S)	10.10
19 X$=$SiH$_2$	0	0	σ(SiSi)	10.98
20 X$=$CH$_2$	0.68		σ(SiC)	12.34
21 X$=$NH	1.35	1.31	*n*(N)	10.70
22 X$=$O	1.53	1.70	*n*(O)	12.36
23 X$=$PH	1.03	1.10	*n*(P), σ(SiP)	9.87
24 X$=$S	1.68	1.52	*n*(S)	10.25
25 X$=$CH$_2$	0.79	0.08	σ(SiSiC)	10.64
26 X$=$NH	1.48	1.22	*n*(N), σ(SiSi)	10.32
27 X$=$O	1.53	1.69	*n*(O), σ(SiSi)	10.87
28 X$=$PH	1.04	1.17	*n*(P), σ(SiSi)	9.53
29 X$=$S	1.53	1.58	*n*(S)	10.21

[a] Dipole moments μ in debye and ionization potentials I in eV are given for the most stable conformation. For **7**–**18**, $\mu > 0$ implies that the positive end of μ points toward the Si, Si midpoint, its negative end toward X. For **19**–**29** only absolute values are given. [b] Experimental values of μ for the corresponding C compounds, HF/6-31G(*d*) values are in general too large by up to 30%. [c] The value of μ is too small due to the large HF/6-31G(*d*) SiOSi angle [46]. Experimental μ: 0.24 debye [25].

SiH bond dipoles are shifted with increasing electronegativity of Y (increasing (HH)SiSi angle, Table 2) in a position almost perpendicular to the C_2 or C_s symmetry element, their contribution to μ becomes smaller. For X = O the SiO bond dipoles dominate thus leading to a relatively large positive value of μ. Similar explanations can be given in the case of μ(**11**) or μ(**12**).

Considering both the magnitude and the direction of the dipole moment in type I compounds, μ for the carbon analogues are more positive for X = NH (HF/6-31G(*d*): 1.95; exp. 1.90 D [48]) and X = O (2.28; 1.89 D [48]) but more negative for X = PH (exp. 1.12 D [48]) and X = S (exp. 1.85 D). Again, this can be explained in terms of a vector model using bond dipoles and considering that (a) CH bond dipoles are much smaller than SiH bond dipoles; (b) the shape of the three-membered ring is different for **9** and **10** than for **2** and **3** (Fig. 2(a), and (c) the direction of the bond dipoles is reversed when going, e.g. from SiP to CP (Fig. 2(b)).

For **14**–**18** μ is more negative than for **8**–**12**. This is caused by two additional SiH bond dipoles pointing away from X. Due to the lower symmetry of type III and type IV compounds, an analysis of calculated dipole moments is somewhat more difficult but can be done along the same lines described above.

Comparison of cyclopropane (1) and cyclotrisilane (7)

The fact that **7** is 11 kcal mol^{-1} more strained than **1** is astonishing since both Baeyer and Pitzer strain should be lower in the Si_3 than the C_3 ring. If Baeyer strain is estimated employing Hooke's law

$$SE(\text{Baeyer}) = 1.5\, k(\text{AAA})\, \{\beta(\text{AAA}) - \beta\ (\text{Reference})\}^2$$

three pieces of information are needed to compare **1** and **7**: the AAA angle (A = C, Si) in the ring, the value of a suitable AAA reference angle, and the AAA bending force constant. The geometrical angle α is of no relevance when discussing Baeyer strain [2,5,7]. Instead the interpath angle β has to be determined and its deviation from the interpath angle of an unstrained reference system has to be considered. For **7**, β(SiSiSi) is calculated to be 81.7° (Table 8), just 3° larger than in **1** (78.7°, Table 8). No matter whether the tetrahedral angle of AH_4 is chosen as a reference angle or the AAA angle of **4** (111.6° [5]) and **13** (112.8°, Table 3), respectively, the difference β(AAA) − β(Reference) is the same for **1** and **7**. The bending force constant, however, is 50% lower for Si (0.55 mdyn Å rad^{-2} [49]) than for C (1.071 mdyn Å rad^{-2} [50]) and resembles that found for CCC bending in the absence of repulsive 1,3 C, C interactions (Dunitz–Shomaker strain, see ref. 7). 1,3 Si, Si interactions seem to be of minor importance as the relatively low SE of cyclotetrasilane (18 kcal mol^{-1} [10]) suggests, i.e. the bending force constant *k*(SiSiSi) has not to be corrected for Dunitz–Shomaker strain [7]. Inserting β(SiSiSi) of **7**, β(Refer-

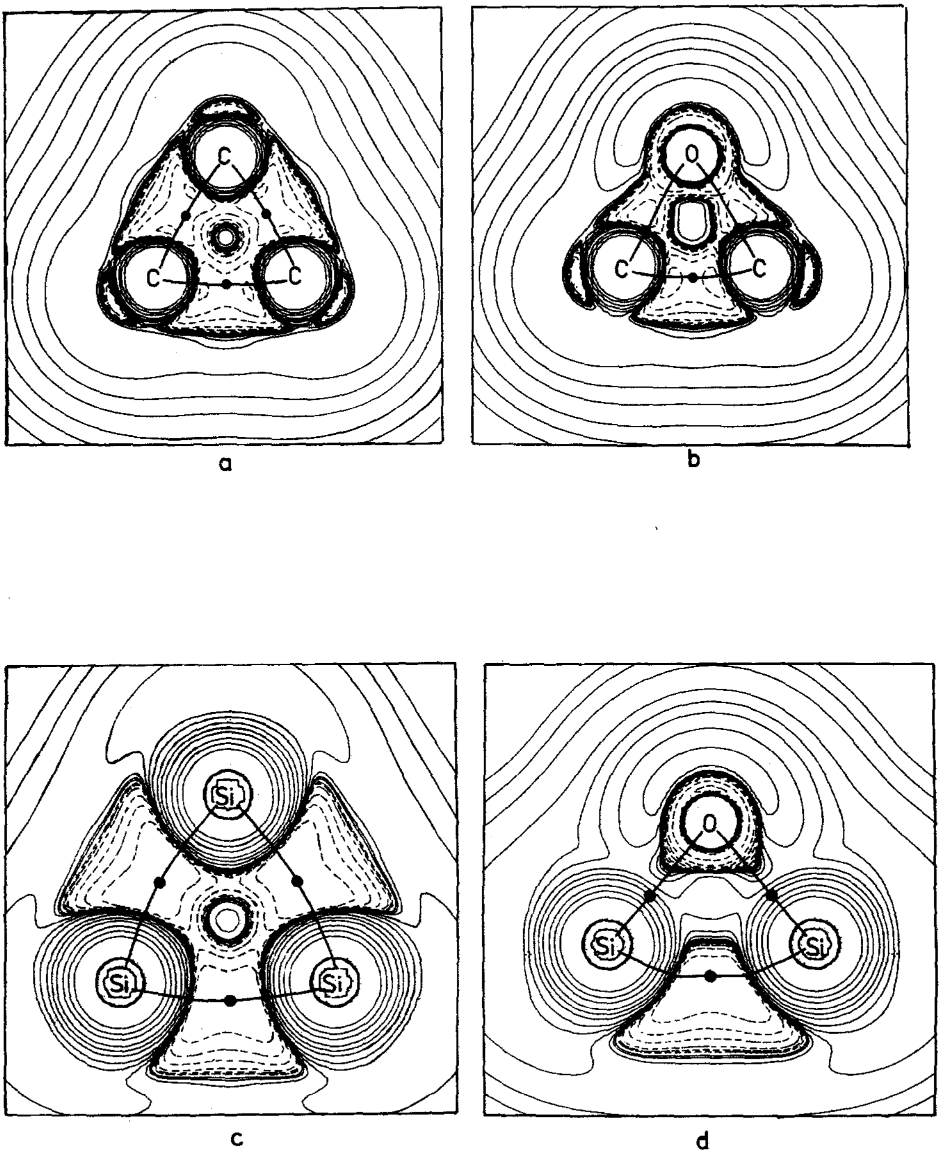

Fig. 3. Bond paths (heavy solid lines), bond critical points (dots) and Laplace concentration $-\nabla^2\rho(\mathbf{r})$ of (a) cyclopropane (**1**), (b) oxirane (**3**), (c) cyclotrisilane (**7**), and (d) disilaoxirane (**10**). The Laplace concentration is given in form of a contourline diagram calculated for the heavy atom plane. Dashed contour lines are in regions with charge concentration ($\nabla^2\rho(\mathbf{r})<0$), and solid lines in regions where negative charge is depleted ($\nabla^2\rho(\mathbf{r})>0$). HF/6-31G(2*d*) calculations.

ence) = 109.5°, and *k*(SiSiSi), angle strain for **7** is calculated to be 28 kcal mol^{-1}.

This value is increased by contributions resulting from SiSiH and HSiH bending. Appropriate bending force constants are 0.61 and 0.41 mdyn Å rad^{-2}, which have been obtained by averaging bending force constants published for **19** [51]. With β(SiSiH) = 114.7 (α = 118.7°) and β(HSiH) = 113.0 (α = 112.7°), angle strain energies of 4.4 and 0.3 kcal mol^{-1} are calculated thus leading to a total Baeyer SE of 32.7 kcal mol^{-1} for **7** (Baeyer SE(**1**) = 41.3 kcal mol^{-1} [7]).

Bond eclipsing in Si_2H_6 leads to an energy increase of 0.9 kcal mol^{-1} [26] (exp. 1.2 kcal mol^{-1} [52]), which is about one third of the energy increase observed for C_2H_6 (exp.: 2.9 kcal mol^{-1} [53]). Accordingly, Pitzer strain of **7** should be one third of that determined for **1** (4 kcal mol^{-1} [7]). Together with the energy for Baeyer strain, a SE of ca. 34 kcal mol^{-1}, 5 kcal mol^{-1} lower than the homodesmotic SE, results.

In a three-membered ring, there are additional factors, which may influence its stability, namely weakening of the ring bonds due to stretching or bending, strengthening of the external ring bonds due to a favorable hybridization at the ring atoms, and a possible stabilization of the ring by an internal 2-electron–3-center bond [2,5,7]. We will discuss the latter factors first.

It is well known that Si has less of a tendency to form sp^n hybrid orbitals than C [54]. As a consequence, Si–Si and Si–H bonds possess more *s* (less *p*) character. For example $sp^{2.1}$ hybrids have been found for the SiH bonds of SiH_4, $sp^{1.9}$ hybrids for those in **7** [10]. Hence, strengthening of the external bonds of a three-membered ring compared to its acyclic counterpart should be less in **7** than in **1**. This is in line with the trends in the calculated CH and SiH bond lengths. The former decrease by 0.012 Å, the latter by 0.007 Å (Table 6) when going from **4** or **13** to the corresponding three-membered ring. With regard to the actual CH and SiH bond lengths, this is a decrease of 1.1 and 0.4% suggesting that SiH bond strengthening stabilizes **7** by just 1–2 kcal mol^{-1}.

Even if the orbitals forming the surface orbital of **7** are sp^2 hybrid orbitals, overlap in the center of the ring should be smaller than in **1** due to the larger size of the Si_3 ring. Accordingly, the internal 2-electron–3-center bond should be less stabilizing and the delocalization of σ-electrons in the ring surface should be reduced. In addition, electrons are withdrawn from the surface orbital in **7** due to the electronegativity difference between H and Si (χ(H) = 2.20; χ(Si) = 1.90). The same effect has been discussed for hexafluoro-**1**, which is 26 kcal mol^{-1} more strained than **1** as a result of the strong σ-acceptor capacity of fluorine [7].

The calculated electron density at the ring critical point (ρ_r = 0.427 for **7**, 1.331 *e* $Å^{-3}$ for **1**, Table 9), the value of η (71 vs. 81%, Table 9), and the bond ellipticities ϵ_b (0.328 vs. 0.455, Table 9), which all reveal that less electron density is smeared out over the ring surface of **7** as compared to **1**, are in line with the predicted reduction of surface delocalization in **7** [7]. This can be visualized when comparing the contour line diagrams of the Laplace concentration calculated for **1** and **7** with regard to the ring plane (see Fig. 3).

Analysis of the bond paths indicates that the ring bonds are different in **1** and **7**. The calculated parameters $Q=11.5$ and $d=0.15$ Å suggest that the bending of the SiSi bond is much stronger than that of the CC bond (6.7 and 0.06, Table 8). Even if one considers that the SiSi bond is almost 60% longer than the CC bond, the computed d value of **7** indicates a strong increase in bending when going from C_3 to Si_3. This is remarkable since the corresponding increase in β is just 3° (Table 8). In the following, we have to investigate whether this is indicative of a qualitative difference between the CC and SiSi bond paths in **1** and **7**.

Optimal bent bonds imply two basic requirements. First, the bond orbitals have to be arranged in such a way that an interpath (interorbital) angle close to that of a strainfree system can be adopted. Secondly, orbitals must support a build-up of density in a region not too far from the internuclear connection line in order to enlarge stabilizing nucleus–electron attraction and to avoid large nucleus–nucleus repulsion.

For **1**, *s,p* hybridization at C leads to sp^5 orbitals [55], which seem to fulfill the two requirements satisfactorily. The local properties of $\rho(r)$ at the CC bond critical points suggest that the CC bonds in **1** are only marginally weaker than those of the acylic reference **4** [5]. For Si, however, hybrid orbitals with high *p* character are not possible (vide infra) and, accordingly, the bond orbitals are too rigid. They support a reasonable interpath angle ($\beta=81.7$, Table 8), but do not allow a build-up of electron density close to the internuclear connection line (d is too large, ρ_b too small, Table 8). According to ρ_b(SiSi), which is 6% lower in **7** than in **13**, the SiSi bonds are weakened in the three-membered ring. Also, they possess less π-character than the corresponding CC bonds (see ϵ_b in Table 9). We conclude that upon bending the strength of the SiSi bond is considerably decreased.

The bond energy of a SiSi single bond has been estimated to be 49 kcal mol^{-1} [56]. Assuming that the decrease in $\rho(r)$ at the SiSi bond critical point reflects a decrease in the bond energy by 6%, a loss of $3\times3=9$ kcal mol^{-1} due to SiSi bond bending can be predicted for **7**. When bond bending strain is added to Baeyer strain (32.7 kcal mol^{-1}), Pitzer strain (1.3 kcal mol^{-1}), and CH bond strengthening (-1 kcal mol^{-1}), a total SE of 42 kcal mol^{-1} is obtained. The difference between this value and the homodesmotic SE of 39 kcal mol^{-1} (Table 10) may be attributed to the stabilizing effect of σ-delocalization in the ring. In this respect, however, a caveat is necessary. If the SiSiSi bending force constant used above is just 15% lower, which is still within the limits of experimental uncertainties, then there will be no need to invoke stabilizing effects by either SiH bond strengthening or σ-delocalization in order to explain the homodesmotic SE of **7**.

We conclude that the change in SE when going from **1** to **7** is caused by an interplay of three, maximally five different effects: (i) SiSi bond weakening due to bending, (ii) a decrease of Baeyer strain, (iii) a decrease of Pitzer strain, (iv) reduced SiH bond strengthening, and (v) reduced σ-delocalization in **7**. Most important is that Si is not able to form sp^n hybrid orbitals with high p character that are needed for the SiSi bent bonds in **7**.

Bent bonds, π-complex character, surface delocalization and ring strain in dependence of X

For II, III, and IV, the ionic character of SiY bonds increases with the electronegativity of Y. Calculated H_b values close to 0 suggest high ionic character for $Y=O$. In the three-membered rings **7–12** the ionic character of SiY bonds is considerably reduced (Table 8). According to computed values $H_b<0$, all ring bonds are covalent bonds.

Bending of the SiSi bond increases in series A: $X=YH_n=SiH_2$, PH, S, CH_2, NH, O, i.e. with increasing electronegativity of Y provided elements Y of the same row of the periodic system are compared. This is reflected by the calculated Q, d, and β values and the Pauling electronegativities χ listed in Table 8. As has been noted above, SiSi distances decrease with $\chi(Y)$ as do SiSi bond path lengths. At the same time angles (HH)SiSi approach 180° (see Table 2), i.e. the geometrical situation adopted in disilene.

Changes in the SiH_2SiH_2 entity of the three-membered ring are coupled with a reduction of the bend of the SiY bonds. For example, both Q and d approach 0 for a large $\chi(X)$ (Table 8). These trends are indicative of a change from convex (outwardly curved) SiY bent bonds to concave (inwardly curved) SiY bent bonds with increasing $\chi(Y)$ [5]. The form of the bent bonds and their dependence on $\chi(Y)$ can be rationalized by donor–acceptor interactions between the group X and the basal group SiH_2SiH_2 [5,8]. The latter donates negative charge from the π MO into a suitable low lying a_1 MO (C_{2v} symmetry assumed) thus establishing a build-up of electron density in the center of the ring. Back donation from a high-lying b_2 MO into the π^* MO of SiH_2SiH_2 leads to a peripheral build-up of electron density, mainly responsible for the curvature of the bond paths (Fig. 4).

Since the π^* MO of disilene is much lower in energy than the π^* MO of ethylene, back donation from X is facilitated in disila rings **7–12**. It leads to a strengthening of the SiX bonds, but a weakening of the SiSi bond.

Actually, when analyzing the electronic structure of a three-membered ring in terms of donor–acceptor interactions between basal and apex group, three rather than one donor–acceptor pairs have to be considered (see Fig. 5). If the basal group is $A=X$ and $\chi(X)>\chi(A)$, then π^* of $A=X$ adopts the form shown in Fig. 5. Overlap between the $p\pi$ orbital of the apex group A and π^* $(A=X)$ is larger in the region AA than the region AX. As a consequence, the bend of

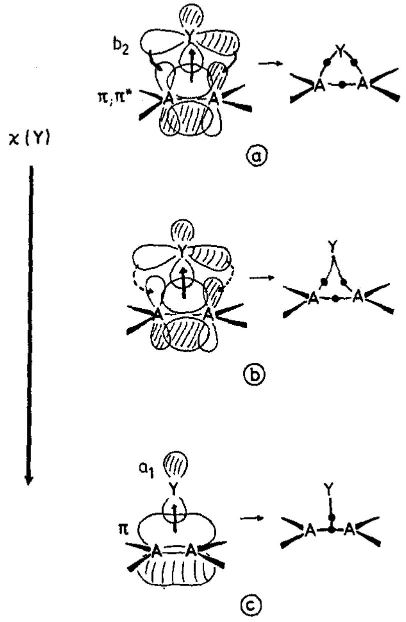

Fig. 4. MO description of donor–acceptor interactions between the basal group A_2H_4 ($A=Si$) and the apex group $X=YH_n$. The relevant orbitals (a_1 and b_2 symmetry) are shown on the left-hand side and the corresponding molecular graphs (bond paths) on the right hand side of each diagram. The direction of charge transfer is indicated by arrows (dashed arrows indicate reduced charge transfer). The Pauling electronegativity $\chi(Y)$ increases from (a) to (c). (a) convex-shaped three-membered ring; (b) concave-shaped three-membered ring; (c) T structure of π-complex.

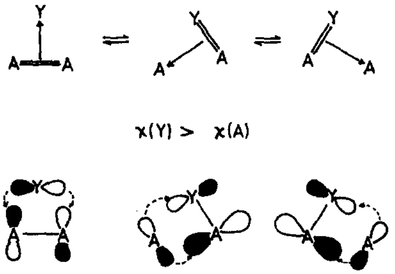

Fig. 5. π-Complex description of a three-membered ring. MOs involved in back-donation are qualitatively shown for the three possible π-complexes. For $\chi(Y) > \chi(A)$, the coefficient of $p\pi(A)$ is larger than that of $p\pi(Y)$ in the $\pi^*(A=Y)$ MO.

the AA bond is more pronounced. Superimposing the three donor–acceptor interactions leads to a strongly bent AA bond and two less strongly bent AX bonds. With increasing electronegativity of X the π^* ($A=X$) MO is more dominated by $p\pi(A)$ and the overlap in the AA region increases as does the bend of the AA bond. This is in line with the observations made when analyzing $\rho(\mathbf{r})$ of **7–12**.

If back donation is reduced in the case of an electronegative X (Y), then the electronic structure of the three-membered ring will approach that of a π-complex, which possesses two coinciding concave "bent bonds" yielding a T structure (Fig. 4). The degree of π-complex character is also revealed by the ellipticity at the ring critical point, ϵ_r (Table 9). The latter increases with $\chi(Y)$ where the direction of the soft curvature given by $\mathbf{v}_r^2$ is always parallel to the SiSi bond as observed for the C analogues [5].

Although the π-complex character increases in series A, none of the three-membered rings considered possesses concave bent bonds ($d<0$), i.e. **7–12** are true rings and, hence, their stability should be analyzed in terms of ring strain, bond (de)stabilization, and surface delocalization [2]. From the discussion of **7** it is clear that both Pitzer strain and SiH bond strengthening make only marginal contributions to the total strain. As for a possible weakening of ring bonds, calculated ρ_b(SiY) values indicate an adjustment of SiY bonds to those of type II compounds in line with their reduced bend (Table 8). For X = PH and S, ρ_b(SiY) is even larger for I than for II. Thus, it seems that upon replacing one SiH_2 group in **7** by X, ring bond weakening is less pronounced.

We conclude that the relative magnitude of the SEs of **7–12** is dominated by changes in Baeyer SEs. Unfortunately, the latter cannot be determined quantitatively since bending force constants k(SiYSi) and k(SiSiY) are not known for most of the hetero atoms Y considered in this work. However, qualitative estimates with regard to the magnitude of Baeyer SEs of type I compounds can be obtained by considering differences $\Delta=\beta(\mathrm{II})-\beta(\mathrm{I})$ ($\Delta=\beta(\mathrm{IV})-\beta(\mathrm{I})$) for angles SiYSi (SiSiY) listed in Table 10. Widening of the angle $\beta(\mathrm{II})\approx\alpha(\mathrm{II})$ is indicative of electrostatic repulsion, possibly d_π–p_π conjugation or other electronic forces, which, of course, are also active in I. High polar (ionic) character of the SiY bonds leads to positive charges at the Si atoms in I and II, a large k(SiYSi) and, hence, relatively large angle and total strain.

The homodesmotic SEs increase in series B from 28–55 kcal mol^{-1} (Table 10): X = S, PH, SiH_2, CH_2, NH, O. If one forms the sum of the Δ values and assumes that Baeyer SE is parallel to this sum, then an ordering similar to series B is obtained (Table 10).

The analysis of computed interpath angles confirms that the homodesmotic SEs are dominated by Baeyer strain. P and S prefer small angles (Table 3) thus leading to total SEs in **11** and **12** lower than that of **7**. For C, N, and O, a compression of angles SiYSi and SiSiY to the values enforced in the three-membered rings is more difficult than in **7** and, therefore, entails large SEs.

Three-membered rings containing Si are at least 10 kcal mol^{-1} more strained than their C analogues. The energies of the SiY bonds with $\chi(Y) > \chi(Si)$ are larger than calculated SE values. Values of 72 and 100 kcal mol^{-1} have been reported for the SiC and the SiO bond respectively [54]. As for the SiSi single bond energy (49 kcal mol^{-1} [56]) the situation is different. Calculated SE values are of comparable magnitude or, as in the case of disilaoxirane (**10**), even larger (by 6 kcal mol^{-1}) than the average SiSi bond energy. This does not imply that **10** is unstable with regard to SiSi bond rupture since the kinetic stability of SiSi bonds is possibly much higher than their thermodynamic stability. For example, the SiSi bond dissociation energy of disilane is known to be 81 kcal mol^{-1} [25], just 7 kcal mol^{-1} lower than the CC bond dissociation energy. Despite the large inherent SEs **7–12** should be sufficiently stable to be observed experimentally.

Owing to the strong bend of the SiSi bond, **7–12** are prone to electrophilic attack, which should be corner-oriented in the first stage of the reaction. An attack at the SiY bond is less likely to lead to a reaction since the SiY bond paths extend less into space (small *d*, Table 8). Also, the corresponding SiY bond are far stronger than the SiSi bond. An attack at an electron lone pair of the group X (X=NH, O, PH, S) is energetically less favorable than attack at the SiSi bond. At least, this is suggested by the calculated ionization potentials listed in Table 11. Contrary to the C analogues, the HOMO in type I compounds is always a SiSi bonding MO even if X possesses a high-lying lone pair orbital. Interaction with an electrophile leads to a charge transfer from the SiSi bonding MO to the LUMO of the electrophile and to a concomitant weakening of the SiSi bond. The first ionization potential of I is 1–2 eV smaller than that of II, III or IV (Table 11) indicating that HOMO–LUMO interactions with an electrophile are facilitated in the three-membered rings **7–12**.

All three-membered rings considered possess a low lying LUMO with SiSi antibonding character. A nucleophilic attack will lead to population of the LUMO and, as a consequence, to SiSi bond rupture. Bulky substituents at the Si atoms hinder both an electrophilic and a nucleophilic attack and, therefore, increase the kinetic stability of type I compounds.

d_π–p_π *conjugation*

In order to explain the geometry of silyl compounds, for example the planarity or near planarity at the N atom of **15**, **21** or **26**, and the large SiOSi and SiOH angle of **16**, **22** or **27**, *dπ–pπ* conjugation between Si and the first row atom Y (Y=N, O) has been invoked [57]. However, recent theoretical investigations have provided convincing evidence that there is no need for *dπ–pπ* conjugation [58]. Bonding features of molecules containing second row elements such as Si can be explained in other ways. For example, the high polarity of the SiN bond leads to a large negative charge at N. Thus, the N center should adopt the geometry of NH_3^-, which according to Walsh's rules prefers planarity [28,59]. Also, electrostatic repulsion between the positively charged bonding partners of N may enforce planarity. A similar explanation can be given for SiOH and SiOSi angle widening in silanol, disiloxane, and related compounds.

In the case of **9**, application of Walsh's rules for a negatively charged N atom, electrostatic effects and the distortion of the ring geometry caused by the size of the N atom (see above) might be considered sufficient to explain planarity at the N atom. However, the analysis of the electron density reveals some bonding features, which could be linked to *dπ–pπ* conjugation. For example, the calculated ellipticity of the NSi bonds is close to zero indicating that electron density is isotropically distributed along the SiN bond path, contrary to the large ellipticity of the CN bond path in **2**. Such an isotropic distribution is obtained when electron density extends into space both in the molecular plane and perpendicular to it. The latter could be due to π-type interactions between the N and the Si atoms. Small ellipticities indicative of an isotropical charge distribution have also been obtained for the SiN and SiO bonds in **10**, **15**, **16**, **21**, **22**, **26**, and **27**, but not for the SiS and the SiP bonds in **11**, **12**, **17**, **18**, etc. Since *dπ–pπ* conjugation in the latter compounds should be more likely than in the former, the calculated SiN and SiO ellipticities provide no unequivocal proof for this type of conjugation.

CONCLUSIONS

Differences between three-membered rings containing Si and those containing C can be traced to the different ability of the two elements to form flexible sp^n hybrid orbitals and to the difference in electronegativities of Si ($\chi=1.90$) and C ($\chi=2.50$). The following points have to be stressed in this connection.

(i) Cyclotrisilane (**7**) is more strained than cyclopropane (**1**) by 11 kcal mol^{-1}, i.e., the SE of **7** is 39 kcal mol^{-1}. The increase in strain is due to SiSi bond bending and the inability of Si to form suitable sp^n hybrid orbitals with high *p* character, which would guarantee flexible bent bond orbitals. Baeyer and Pitzer strain are lower in **7** than in **1**. Strengthening of the external SiH bonds and σ-delocalization in the Si_3 ring is negligible in **7**.

(ii) Replacement of a SiH_2 group by CH_2, NH, O leads to an increase in SE by 3.8, 4.1 and 19.1 kcal mol^{-1}, a replacement by PH or S to a decrease in SE by 4.8 and 10.8 kcal mol^{-1}, respectively. This is due to changes in Baeyer strain as revealed by a comparison of interpath angles both for the three-membered rings and the reference compounds shown in Scheme 1.

(iii) The π-complex character of type I compounds increases with increasing Pauling electronegativity $\chi(Y)$. This is revealed by the bending of the SiSi bond and the SiY bonds.

(iv) The disila rings I are prone to electrophilic attack at the SiSi bond, which should be easily broken. This is suggested by the calculated density distribution and the nature of the HOMO, which is a SiSi bonding MO. Breaking of the SiY bond is less likely since the bond strength increases with $\chi(Y)$.

ACKNOWLEDGEMENTS

We thank Prof. R. West for conveying experimental results prior to publication and for suggesting this work. This work was supported by the Deutsche Forschungsgemeinschaft and the Fonds der Chemischen Industrie. All calculations were done at Rechenzentrum der Universität Köln.

NOTE ADDED IN PROOF

After this paper had been submitted, R. West and co-workers (H.B. Yokelson, A.J. Millevolte, G.R. Gillette, and R. West, J. Am. Chem. Soc., 109 (1987) 6865) reported the synthesis and crystal structure of tetramesityldisilaoxirane. The X-ray structural data of this compound (R(SiSi) = 2.227; R(SiO) = 1.733 Å; SiSiO = 50.0; SiOSi = 80.0°) confirm predictions made for the parent disilaoxirane in this paper. Synthesis, structural data, and bonding features of Si-containing three-membered rings have recently been reviewed by R. West in Angew. Chem., 99 (1987) 1231. Also, R.S. Grev and H.F. Schaefer III, J. Am. Chem. Soc., 109 (1987) 6569, 6577 published DZ+P energies, geometries, and harmonic frequencies for a set of Si containing molecules similar to that discussed in this work.

REFERENCES

1 (a) L. Pauling, The Nature of the Chemical Bond, 3rd edn., Cornell University Press, Ithaca, NY, 1960.
  (b) L. Pauling, J. Am. Chem. Soc., 53 (1931) 1367.

2 For a recent review, see D. Cremer and E. Cremer, Scope and Limitations of the Concept of Strain in J.F. Liebman and A. Greenberg (Eds.), Molecular Structure and Energetics, VCH, Deerfield Beach, FL, Vol. 6 in press.

3 (a) A. Greenberg and J.F. Liebman, Strained Organic Molecules, Academic Press, New York, 1978.
  (b) J.F. Liebman and A. Greenberg, Chem. Rev., 76 (1976) 311.
  (c) M.D. Newton, in H.F. Schaefer III (Ed.), Applications of Electronic Structure Theory. Vol. 4. Plenum Press, New York, 1977.
  (d) K.B. Wiberg, Angew. Chem. Int. Ed. Engl., 25 (1986) 312.
  (e) S.W. Benson, Thermochemical Kinetics, Wiley, London, 1976.

4 (a) M.J.S. Dewar, J. Am. Chem. Soc., 106 (1984) 669.
  (b) M.J.S. Dewar, Bull. Soc. Chem. Belg., 88 (1979) 957.
  (c) M.J.S. Dewar and M.L. McKee, Pure Appl. Chem., 52 (1980) 1431.

(d) The idea that cyclopropane is isoconjugate with benzene can already be found in early PPP calculations. See R.D. Brown and V.G. Krishna, J. Chem. Phys., 45 (1966) 1482.
5 D. Cremer and E. Kraka, J. Am. Chem. Soc., 107 (1985) 3800.
6 D. Cremer and E. Kraka, J. Am. Chem. Soc., 107 (1985) 3811.
7 D. Cremer and J. Gauss, J. Am. Chem. Soc., 108 (1986) 7467.
8 M.J.S. Dear and G.P. Ford, J. Am. Chem. Soc., 101 (1979) 183.
9 (a) A.F. Sax, Chem. Phys. Lett., 127 (1986) 163; Chem. Phys. Lett., 129 (1986) 66.
(b) A.F. Sax and J. Kalcher, J. Chem. Soc. Chem. Commun. (1987) 809.
10 (a) P.v.R. Schleyer, NATO AST Ser. C, 189 (1986) 69.
(b) P.v.R. Schleyer, A.F. Sax, J. Kalcher and R. Janoschek, Angew. Chem., 99 (1987) 374.
11 W.W. Schoeller and T. Dabisch, J. Chem. Soc. Chem. Commun., 1985, 1706. These authors claim that the SEs of **1** and **7** are about equal. However, their claim is based on isodesmic, rather than homodesmotic, reaction energies.
12 S. Nagase, M. Nakano and T. Kudo, J. Chem. Soc. Chem. Commun., (1987) 60.
13 S. Masamune, Y. Hanzawa, S. Murakami, T. Bally and J.F. Blount, J. Am. Chem. Soc., 104 (1982) 1150.
14 H. Watanabe, T. Okawa, M. Kato and Y. Nagai, J. Chem. Soc. Chem. Commun., (1983) 781.
15 H. Watanabe, M. Kato, T. Okawa and Y. Nagai, J. Organomet. Chem., 271 (1984) 225.
16 A. Schäfer, K.P. Weidenbruch and H.G. von Schnering, Angew. Chem., 96 (1984) 311.
17 J.C. Dewan, S. Murakami, J.T. Snow, S. Collins and S. Masamune, J. Chem. Commun., (1985) 892.
18 D. Seyferth and D.P. Duncan, J. Organomet. Chem., 111 (1976) C21.
19 M. Ishikawa, M. Sugisawa, M. Kumada, T. Higuchi, K. Matsui, K. Hirotsu and J. Iyoda, Organometallics, 2 (1983) 174.
20 S. Masamune, S. Murakami and H. Tobita, J. Am. Chem. Soc., 105 (1983) 7776.
21 M. Ishikawa, S. Matsuzawa, H. Sugisawa, G. Yano, S. Kamitori and T. Higuchi, J. Am. Chem. Soc., 107 (1985) 7706.
22 M.J. Michalczyk, R. West and J. Michl, J. Chem. Soc. Chem. Commun., (1984) 1525.
23 R. West, J.D. De Young and K.J. Haller, J. Am. Chem. Soc., 107 (1985) 4942.
24 R. West, personal communication.
25 For a discussion of theoretical calculations on types II-IV compounds up to 1981 see E. Hengge, H. Keller-Rudek, D. Koschel, U. Krüerke and P. Merlet, Silicon, Gmelin Handbook of Inorganic Chemistry, Supplement Volume B1, 1982, Springer, Berlin.
26 B.T. Luke, J.A. Pople, M.-B. Krogh-Jesperson, Y. Apeloig, J. Chandrasehhar and P.v.R. Schleyer, J. Am. Chem. Soc., 108 (1986) 260.
27 (a) A. Komornicki, J. Am. Chem. Soc., 106 (1984) 3114.
(b) W.J. Pietro, M.M. Francl, W.J. Hehre, D.J. De Frees, J.A. Pople and J.S. Binkley, J. Am. Chem. Soc., 104 (1982) 5039.
(c) A.F. Sax, J. Comput. Chem., 6 (1985) 469.
28 (a) M.S. Gordon, Chem. Phys. Lett., 126 (1986) 451.
(b) C. Glidewell and C. Thomson, J. Comput. Chem., 3 (1982) 495.
29 C. Glidewell and C. Thomson, J. Comput. Chem., 4 (1983) 9.
30 (a) H. Oberhammer and J. Boggs, J. Am. Chem. Soc., 102 (1980) 7241.
(b) J. Sauer and B. Zurawski, Chem. Phys. Lett., 65 (1979) 587.
(c) J. Sauer, P. Hobza and R. Zahradnik, J. Phys. Chem., 84 (1980) 3318.
(d) S. Grigorias and T.H. Laue, J. Comput. Chem., 8 (1987) 84.
31 (a) M.M. Francl, W.J. Pietro, W.J. Hehre, J.S. Binkley, M.S. Gordon, D.J. De Frees and J.A. Pople, J. Chem. Phys., 77 (1982) 3654.
(b) P.C. Hariharan and J.A. Pople, Theor. Chim. Acta, 28 (1973) 213.
(c) M.S. Gordon, Chem. Phys. Lett., 76 (1980) 163.

32 W.J. Hehre, L. Radom, P.v.R. Schleyer and J.A. Pople, Ab initio Molecular Orbital Theory, Wiley, New York, 1986.

33 (a) C. Møller and M.S. Plesset, Phys. Rev., 46 (1934) 618.
(b) J.A. Pople, J.S. Binkley and R. Seeger, Int. J. Quantum Chem. Symp., S10 (1976) 1.

34 (a) P. George, M. Trachtman, C.W. Bock and A.M. Brett, Tetrahedron, 32 (1976) 317.
(b) P. George, M. Trachtman, C.W. Bock and A.M. Brett, Theor. Chim. Acta, 38 (1975) 121.

35 (a) W.J. Hehre, R. Ditchfield, L. Radom and J.A. Pople, J. Am. Chem. Soc., 92 (1970) 4796.
(b) L. Radom, W.J. Hehre and J.A. Pople, J. Am. Chem. Soc., 93 (1971) 289.

36 M.J. Frisch, J.A. Pople and J.S. Binkley, J. Chem. Phys., 80 (1984) 3265.

37 (a) R.F.W. Bader, T.S. Slee, D. Cremer and E. Kraka, J. Am. Chem. Soc., 105 (1983) 5061.
(b) D. Cremer, E. Kraka, T.S. Slee, R.F.W. Bader, C.D.H. Lau, T.T. Nguyen-Dang and P.J. MacDougall, J. Am. Chem. Soc., 105 (1983) 5069.

38 D. Cremer and E. Kraka, Croat. Chem. Acta, 57 (1985) 1265.

39 D. Cremer and E. Kraka, Angew. Chem. Int. Ed. Engl., 23 (1984) 627.

40 D. Cremer, New Ways of Analyzing Chemical Bonding, in Z.B. Maksic (Ed.), Modelling of Structure and Properties of Molecules, Ellis Horwood, Chichester, 1987, p. 125.

41 Bader uses the term "bond path" for any MED path resulting from interactions between atoms. Since we want to distinguish between the various atom–atom interactions, the term "bond path" is used in this work only for covalent bonds. See, e.g., R.F.W. Bader, T.T. Nguyen-Dang and Y. Tal, Rep. Prog. Phys., 44 (1981) 893.

42 R.F.W. Bader and H. Essen, J. Chem. Phys., 80 (1984) 1943.

43 R.F.W. Bader, P.J. MacDougall and C.D.H. Lau, J. Am. Chem. Soc., 106 (1984) 1594.

44 W. Koch, G. Frenking, J. Gauss, D. Cremer and J.R. Collins, J. Am. Chem. Soc., 109 (1987) 5917.

45 For example the dependence of the SiSi bond length on steric repulsion is obvious in the case of hexa-tert-butyl disilane. See N. Wiberg, H. Schuster, A. Simon and K. Peters, Angew. Chem., 98 (1986) 100.

46 At the HF/6-31G(*d*) level, standard exponents for the *d* functions lead to SiOSi angle of 171°. A better value is obtained by reducing the exponent for Si to about 0.3. See ref. 31(b). The experimental geometry is: R(SiO) 1.634; R(SiH) 1.486 Å; ∠(SiOSi) 144.1°. See A. Almeningen, O. Bastinansen, V. Ewing, K. Hedberg and M. Traetteberg, Acta Chem. Scand., 17 (1963) 2455.

47 (a) R. Walsh, Acc. Chem. Res., 14 (1981) 246.
(b) M.W. Chase, J.L. Curnutt, R.A. MacDonald and A.N. Syvernud, J. Phys. Chem. Ref. Data, 7 (1978) 793.

48 (a) R.D. Nelson, D.R. Lide and A.A. Maryott, Selected Values of Electric Dipole Moments for Molecules in the Gas Phase, NSRDA-NBS 10, U.S. Government Printing Office, Washington D.C., 1967.
(b) McClellan Tables of Experimental Dipole Moments, Freeman, San Francisco, 1963; Vol. 2, Rahara Enterprises, El Cerrito, CA, 1974.

49 (a) F. Höfler, G. Bauer and E. Hengge, Spectrochim. Acta, Part A,32 (1976) 1435.
(b) K. Hassler, E. Hengge and D. Kovar, Spectrochim. Acta, Part A,34 (1978) 1193.

50 (a) R.G. Snyder and J.M. Schachtschneider, Spectrochim. Acta, 21 (1965) 169.
(b) R.G. Snyder and G. Zerbi, G. Spectrochim. Acta, Part A, 23 (1967) 391.

51 (a) J.L. Duncan, Spectrochim. Acta, 20 (1964) 1807.
(b) E.A. Clark and A. Weber, J. Chem. Phys., 45 (1966) 1759.
(c) M. Pfeiffer and H.-J. Spangenberg, Z. Physik. Chem. (Leipzig), 232 (1966) 47.
(d) K. Venkateswarlu and A. Natarajan, J. Chem. Phys., 66 (1969) 1318.

52 J.R. Durig and J.S. Church, J. Chem. Phys., 73 (1980) 4784.

53 S. Weiss and G. Leroi, J. Chem. Phys., 48 (1968) 962.

54 W. Kutzelnigg, Angew. Chem., 96 (1984) 262.
55 (a) M. Randić and Z.B. Maksić, Theor. Chim. Acta, 3 (1965) 59.
(b) See also Ref. 3(c).
56 (a) A.E. Beeser and C.T. Mortimer, J. Chem. Soc. A, (1966) 514.
(b) See also P. Potzinger, A. Ritter and J. Krause, J.Z. Naturforsch., Teil A, 30 (1975) 347.
57 For a summary of arguments relevant to d_π-p_π conjugation see ref. 25.
58 See, e.g. the discussion in refs. 26 and 28.
59 B.M. Gimarc, Molecular Structure and Bonding, Academic Press, New York, 1979.